View metadata, citation and similar papers at core.ac.uk

brought to you by CORE

provided by NASA Technical Reports Server

NASA Reference Publication 1195

1987

Nuclear Techniques in Studies of Condensed Matter

Jag J. Singh

Langley Research Center
Hampton, Virginia

National Aeronautics and Space Administration

Scientific and Technical Information Division

Summary

Nuclear techniques have played an important role in the studies of materials over the past several decades. For example, X-ray diffraction, neutron diffraction, neutron activation, and particle- or photon-induced X-ray emission techniques have been used extensively for the elucidation of structural and compositional details of materials. Several new techniques have recently been developed. In this report, we have briefly reviewed four techniques which have great potential in the study and development of new materials. Of these four, Mössbauer spectroscopy, muon spin rotation, and positron annihilation spectroscopy techniques exploit their great sensitivity to the local atomic environment in the test materials. Interest in synchrotron radiation, on the other hand, stems from its special properties, such as high intensity, high degree of polarization, and high monochromaticity. It is hoped that this brief review will stimulate interest in the exploitation of these newer techniques for the development of improved materials.

Introduction

Nuclear techniques are widely used in several branches of science, including biomedicine, chemistry, industrial hygiene, structural materials, polymer science, and fluid dynamics. Their applications in studies of condensed matter have been particularly fruitful. In this review, we briefly summarize the various techniques that are currently used in condensed matter studies. These techniques can be divided into two broad groups. The first group includes the older, more established techniques that have been in use for several decades. Among the more important techniques in this group are charged-particle scattering and activation, neutron scattering and activation, and photon-induced X-ray emission. The second group includes more recent, emerging techniques that are now finding their place in the arsenal of the experimental materials scientists. The following techniques fall into this category: (1) Mössbauer spectroscopy,[1] (2) muon spin rotation, (3) positron annihilation spectroscopy, and (4) synchrotron radiation research. A brief description of the various techniques follows, with special emphasis on the more recent methods.

[1] We have included Mössbauer spectroscopy in this group because its unique and sensitive applications in engineering materials studies have only recently been recognized.

Nuclear Techniques

Early Techniques

One of the earliest uses of nuclear techniques in materials science involves nondestructive analysis of test materials using nuclear radiation (i.e., particles, gamma rays, and X-rays). Charged-particle interactions with matter include both elastic and inelastic scattering processes. Elastic scattering cross section depends on the level scheme and atomic number of the scattering nucleus. Figure 1 (from ref. 1) shows proton elastic scattering cross section from three isotopes of cadmium as a function of energy. Figure 2 (from ref. 2) shows elastic scattering cross section at 40 MeV as a function of the scattering angle for three different elements. Figure 3 (from ref. 2) shows the pulse-height spectrum of protons scattered from a thin nickel target. Besides the elastic peaks from nickel and trace impurities (C^{12}, O^{16}, Si^{28}, and Fe^{56}), a large number of inelastic peaks from Ni^{64} are shown. Figure 4 (from ref. 3) shows another scattered proton spectrum from an aerosol sample. Besides the elastic peaks from several elements resulting from strong resonances in the (p + element) system, it shows an inelastic peak corresponding to the first excited state in Na^{23}. The simultaneous presence of elastic and inelastic peaks from certain scatterer atoms provides added evidence for their presence in the sample. The charged particle activation (CPA) technique is also appropriate for the detection of lighter elements in the target material. Sometimes different nuclear reactions in different impurity elements can lead to the excitation of the same residual nuclear states, and this creates interferences in the activation spectra. However, use of several incident energies—coupled with an appropriate choice of nuclear reactions—can often resolve these difficulties. For example, boron and nitrogen interferences can be resolved by using $B^{10}(d,n)C^{11}$ and $N^{14}(d,\alpha n)C^{11}$, reactions for which relative cross section ratio changes from 30 to infinity as the deuteron energy decreases from 10.0 to 5.9 MeV (ref. 3).

Besides the techniques mentioned above, there are Rutherford backscattering (RBS) and proton-induced X-ray emission (PIXE) techniques that have frequently been used for detecting trace concentrations of contaminant atoms in materials of environmental and technological interest. These techniques have been extensively reviewed in references 4 to 8. Helium-induced hydrogen recoil and resonant $H^1(N^{15}, \alpha\gamma)C^{12}$ and $H^1(F^{19},\alpha\gamma)O^{16}$ nuclear reaction analyses have been used to study hydrogen depth profile in solids (refs. 9 to 14). The problems which can be studied with these latter techniques include the diffusion of hydrogen inside solids, the

chemisorption of hydrogen on surfaces, and the radiation damage distribution caused by the low-energy beams of hydrogen. The last application is of particular interest in the field of fusion research.

Neutrons also interact with matter by elastic and inelastic scattering processes and capture reactions. Higher energy neutrons generally produce lattice displacements and secondary atoms throughout the irradiated volume. Thermal neutrons may be captured by the target nuclei to form radionuclides, which subsequently decay by characteristic nuclear gamma-ray emissions. It is the thermal neutrons that form the basis of the bulk of neutron applications to materials science. They have been used extensively for compositional analysis and radiographic inspection of materials. Thermal neutrons have a wavelength which peaks around 1.6 Å, well suited for analyzing variations in the atomic density on a microscopic scale. Because of their magnetic properties, neutrons are also ideally suited for the study of magnetic structures and short-wavelength magnetic fluctuations, such as spin waves. Small-angle neutron scattering (SANS) is another application of low-energy neutrons for studying and characterizing defects in metals, semiconductors, and glasses. It can be used to detect very small (0.01 to 0.10 μm) defects, which can be related to their sites of nucleation and consequently to the mechanisms responsible for modifying properties of materials (ref. 15). For a detailed review of neutron scattering in condensed-matter physics, see references 16 to 18 and references cited therein.

Neutron diffraction has recently become a powerful tool for studying the structure of polycrystalline materials. Because of high neutron sensitivity to oxygen atoms, neutron diffraction is currently providing a comparatively unambiguous picture of where the oxygen atoms are in the newly discovered high-temperature superconductors (ref. 19). The combination of highly developed X-ray methodology with the penetrating power of thermal neutrons offers the potential for determination of general stress states and stress variations through the bulk of the solid materials (refs. 20 and 21).

Like charged particles, photons can also remove inner shell electrons from the target atoms, resulting in subsequent characteristic X-ray emission. Photon-induced X-ray emission has been used widely in material composition analysis. High-energy photons can also induce nuclear reactions in the target atoms. Some elements—such as Be, C, N, and Pb—which are not highly activated with thermal neutrons (ref. 3) can be more conveniently studied with instrumental photon activation analysis (IPAA). Sometimes interferences experienced in neutron activation analysis can be avoided by using IPAA. For example, determination of nickel may be complicated by $Ni^{64}(n,\gamma)Ni^{65}$ and $Cu^{65}(n,p)Ni^{65}$ interferences in the neutron activation spectra. However, the photonuclear reaction product Ni^{57} produced in the $Ni^{58}(\gamma,n)Ni^{57}$ reaction cannot be produced from any other element at photon energies less than 45 MeV. The IPAA technique is equally applicable to geochemical, biological, and oceanographic samples. In general, however, IPAA is not as sensitive as charged-particle and neutron activation analyses.

Recent Techniques

There are several prominent techniques in this group. We discuss four of them in some detail here.

Mössbauer spectroscopy. Mössbauer spectroscopy (MS) is a rather recent technique, having been discovered only in 1958. It is based on the fact that the recoil energy imparted to a nucleus by the emission of a low-energy gamma ray is not always larger than the lattice vibration energies (10^{-2} to 10^{-1} eV) of the atoms. When the recoil energy E_R is much less than the lattice vibration energy $n\hbar\omega$, the fraction of emission events without any loss of energy f (ref. 22) can be calculated as follows:

$$f = \exp(-\kappa^2\langle x^2\rangle) \tag{1}$$

where κ is the wave number of the emitted radiation and $\langle x^2\rangle$ is the mean square amplitude of vibration of the emitter atom along the direction of emission of the gamma ray averaged over the Mössbauer level lifetime. Clearly, when the emitting nucleus is not bound to the lattice, $\langle x^2\rangle$ is usually so large as to make the recoiless fraction f essentially zero. Equation (1) can be extended to three dimensions by using the Debye approximation

$$f = \exp\left(-\frac{\kappa^2\langle r^2\rangle}{3}\right) \tag{2}$$

where

$$\langle r^2\rangle = \frac{9\hbar^2}{4Mk\theta_D}\left(1 + 4\frac{T^2}{\theta_D^2}\int_0^{\theta/T}\frac{u\,du}{e^u - 1}\right) \tag{3}$$

and

$$u = \left(\frac{\hbar\omega}{kT}\right)$$

Equation (3) can be simplified as follows:

$$\langle r^2\rangle = \frac{9E_R}{2k\theta_D\kappa^2}\left(1 + \frac{2\pi^2T^2}{3\theta_d^2}\right) \qquad \left(\frac{\theta_D}{T} >> 1\right) \tag{4}$$

where k is the Boltzmann constant and θ_D is the Debye temperature. Equation (2) shows that the Mössbauer effect cannot take place in liquid, except in highly viscous solutions when $\langle r^2 \rangle$ is bounded. The Mössbauer effect can take place in both crystalline and amorphous solids. It has been used extensively in studies in solid-state physics, physical metallurgy, coordination chemistry, organometallic compounds, and the role of iron in biological systems. The basis of all these diverse applications is the sensitive interaction between the Mössbauer nucleus and its neighbors. Changes in the atomic environment of the Mössbauer nuclei are reflected in the magnitudes of various Mössbauer parameters, such as isomer shift, hyperfine field interaction, and quadrupole splitting.[2] For example, isomer shift δ (refs. 22 to 24) is given by

$$\delta = \frac{2\pi}{5} Z e^2 \left(R_{\text{ex}}^2 - R_{\text{gd}}^2 \right) \left[\psi_A^2(0) - \psi_S^2(0) \right] \qquad (5)$$

where R_{ex} is the nuclear radius in the excited state, R_{gd} is the nuclear radius in the ground state, and $\psi_A(0)$ and $\psi_S(0)$ are the ground-state wave functions of the absorber and source nuclei. If we have a well-characterized standard source, δ-values for the test absorber will simply be determined by their $\psi_A^2(0)$-values.

The effective magnetic field at the absorber nucleus H_{eff}, determined by the electron charge distribution around it, is extremely sensitive to local structural and chemical fluctuations. It can thus serve as a highly useful probe for characterizing solids (refs. 25 to 27).

When the charge distribution inside the Mössbauer nucleus is not spherically symmetrical, it can interact with the gradient of the electric field (EFG) around it because of other charges in the crystal. The interaction between the nuclear quadrupole moment Q and the EFG q (ref. 28) is given by the following expression:

$$E_Q = \frac{eqQ}{4I(2I-1)} \left[3I_z^2 - I(I+1) \right] \left(1 + \frac{\eta^2}{3} \right)^{1/2} \qquad (6)$$

where

$$q = \left(\frac{\partial^2 V}{\partial z^2} \right)$$

$$\eta = \left[\frac{(\partial^2 V/\partial x^2) - (\partial^2 V/\partial y^2)}{(\partial^2 V/\partial z^2)} \right] \qquad (0 \le \eta \le 1)$$

Clearly, any changes in q and η are reflected in the E_Q-values.

Figure 5 shows a conventional constant-acceleration Mössbauer spectroscopy system. The radioactive source (5 to 25 mCi) is moved at a constant acceleration with respect to the absorber in the velocity range of a few millimeters per second to a few centimeters per second. The absorber temperature may be varied depending on the purpose of the study. The Mössbauer radiation may be detected in the transmission or backscattering mode and is recorded with a multichannel analyzer. The source and the absorber must have a common Mössbauer nucleus, such as Fe^{57}, Sn^{119}, or Eu^{151}. Typical Mössbauer spectra are shown in figures 6(a) (from ref. 29) and 6(b) (from refs. 25 to 27).

Some of the interesting applications of Mössbauer spectroscopy have been in the fields of magnetism and chemical physics. (See refs. 30 to 34.) Another important application (ref. 35) has been the study of solid surfaces. Through the use of conversion electron spectroscopy, the surface composition of steels, surface stress, and other thin film properties can be investigated. Other investigations have included measurements of oxidation and corrosion of iron-bearing solids in a variety of gaseous atmospheres. An application of contemporary technological interest relates to the study of hydrogen storage materials (ref. 36). Many intermetallic compounds of d- and f-shell elements reversibly absorb large amounts of hydrogen at easily accessible temperatures and pressures. Mössbauer spectroscopy is a particularly powerful means by which the chemical nature of hydrogen and its location in the ternary hydrides may be identified. Another current application relates to the elucidation of the electronic structure of the rare earth ion in the quarternary-phase high-temperature superconductor $Ba_2EuCu_3O_{7.1}$. The trivalent charge on the rare earth ion in combination with a divalent charge for Ba and the observed oxygen stoichiometry results in an appropriate copper oxidation state for metallic conductivity (ref. 37). For more detailed reviews of the use of Mössbauer spectroscopy in materials science, see references 38 and 39.

[2] Hyperfine field interaction is almost an order of magnitude more sensitive to changes in the chemical surroundings than the isomer shift and quadrupole interaction.

Muon spectroscopy. Muons are excellent probes for local magnetic structure for the condensed phase of matter. Muons are produced in the decay of pions and, like the neutrinos produced at the same time, have negative helicity. This fact ensures easy generation of almost 100-percent-polarized muon beams. The muons quickly come to rest in solids in 0.01 to 0.10 ns, preserving most of their polarization. (The degree of polarization preservation varies with the stopping medium, as shown subsequently.) The stopped muons eventually decay via a parity nonconserving weak interaction with an angular distribution of the form (refs. 40 and 41)

$$\frac{dN_e}{d\Omega} = A(1 + a\cos\theta) \tag{7}$$

where a is the decay asymmetry parameter and θ is the angle between the muon spin and the emitted electron. The decay electron distribution thus reflects the direction of the muon magnetic moment at the time of its decay.

The muon spectroscopy (of which there are several variations) consists basically of starting a clock when a spin-polarized muon enters a sample, stopping it when its decay electron is observed in a given direction, and accumulating these events in a histogram of number of events as a function of the $(\mu - e)$ time interval. The muons are produced in copious quantities in medium- and high-energy accelerators specializing in the production of relatively low-energy pion beams. The pion decays produce a beam of spin-polarized muons. Prominent meson-producing facilities include SIN, TRIUMF, LAMPF, and BNL.

In a vast majority of experiments, it is the positive muons μ^+ produced in the decay of positive pions π^+ that provide the muon spin rotation experimental beams. When a polarized μ^+ is stopped in the test target, it precesses in the local internal magnetic field with a Larmor frequency determined by its magnetic moment. If the target is an insulator or a semiconductor, a muonium μ^+e^- is sometimes formed which then precesses with a frequency determined by the muonium magnetic moment. Studies of muon precession frequency spectra show considerable promise in the characterization of samples prepared by different techniques of current technological interest.

Muon spin rotation (μ^+SR) experiments[3] can be conducted with zero field and with transverse or parallel external fields. For transverse external fields, the stopped muons undergo Larmor precession in a plane perpendicular to the magnetic field. Eventually, the muons decay and the positrons are detected in some fixed direction with respect to the initial polarization. The time histogram of the decaying muons (refs. 42 and 43) can be written as follows:

$$N(t) = N_o \exp(-t/\tau_\mu^+)\left(1 + aG_\perp(t)\ \cos(\omega t + \theta)\right) + B \tag{8}$$

where τ_μ^+ is the μ^+ lifetime, ω is the μ^+ angular precession frequency, and $G_\perp(t)$ is the time-dependent depolarization function in a transverse ($\perp$) magnetic field. The $G_\perp^{(t)}$ may often be approximated[4] as follows:

$$G_\perp(t) = \exp\left\{-\sigma^2\tau_c^2\left[\exp(-t/\tau_c) - 1 + \frac{t}{\tau_c}\right]\right\} \tag{9}$$

where σ is the width of the static local frequency distribution and τ_c is the local field correlation time, which approximately equals the muon jump time.

Typical μSR data (e.g., ref. 44) are illustrated in figure 7. The two most important quantities measured by this technique are the precession frequency ω and the depolarization rate. Both are strongly dependent on the local defect and impurity concentrations in the test solid.

For parallel fields, the quantity measured is the depolarization of the muon spin ensemble. The depolarization function $G_\parallel(t)$ (refs. 45 to 47) is given by

$$G_\parallel(t) = \left[\frac{N_F(0) + N_B(0)}{N_F(0) - N_B(0)}\right]\left[\frac{N_F(t) - N_B(t)}{N_F(t) + N_B(t)}\right] \tag{10}$$

where N_F and N_B are the intensities of the decay positrons in the forward and backward directions. The effect of a longitudinal field on the depolarization function provides useful information about the depolarization mechanism.

The μSR has proved to be a very useful new probe for condensed matter. Several studies have shown that the muon provides unique information[5]

[3] The μSR acronym, analogous to ESR and NMR, has been used for muon spin rotation, relaxation, resonance, and research. Any study of the interaction of the muon spin by virtue of the asymmetric decays is considered μSR.

[4] This "Abragamian" form is valid for a Gaussian local field distribution and an exponential magnetic-field time autocorrelation function.

[5] Mössbauer spectroscopy and μSR can provide complementary information about the effects of

about the magnetic and electronic structure of solids (ref. 48). The discovery by μSR of large internal magnetic fields for the spin-freezing type of ordering (refs. 49 and 50) in spin glasses proved very useful in the formulation of the theory of these dilute magnetic alloys. Muon studies of metals have revealed the presence of microscopic impurity clusters, thus providing a new basis for understanding the effects of impurity correlations in metals. The μSR studies have provided a better understanding of the hydrogen embrittlement phenomenon in steels and other structural alloys, since the behavior of muons in metals is similar to that of hydrogen (ref. 51). One new area where μSR will play a significant role concerns superconductors, particularly the newly developed high-temperature ceramic superconductors (refs. 52 to 55). Previous studies of the superconductors (refs. 56 and 57) in the mixed states have given mixed results. Concurrent μSR studies of the old and new superconductors should be particularly useful in helping to develop theoretical models for the high-temperature superconductivity.

Positron annihilation spectroscopy. Positrons are antiparticles of electrons. They are slowed down quickly upon entering a condensed medium. They may annihilate as free positrons after thermalization or after being trapped at defect sites or in microvoids. In insulators and organic compounds, some of the trapped positrons form a loose assembly with the available electrons to form positronium (Ps) atoms. Depending on the final states in which the positrons find themselves, they annihilate at different times. The time and manner of annihilation of the positrons can thus provide valuable information about the electronic and physical structure of the bulk material and various defects and other impurity centers in it.

Positron annihilation spectroscopy (PAS) involves three different types of measurements: lifetime, Doppler broadening, and angular correlation measurements. The lifetime measurements make use of the fact that the probability for positron annihilation depends on the electron density in the vicinity of the annihilating positrons. The Doppler broadening and angular correlation measurements, on the other hand, are based on conservation of energy and momentum in the positron annihilation process. Because of the nonzero momentum of the annihilating pairs, the resulting gamma rays are emitted with energies equal to $m_0C^2 \pm \Delta E$ and in the directions $180 \pm \Delta\theta$. The probabilities of various values of ΔE and $\Delta\theta$ are the bases for Doppler broadening and angular correlation measurements, respectively. These measurements can provide detailed information regarding the electron momentum states in the test materials.

A typical positron-lifetime measurement system is shown in figure 8. Positron-emitting radionuclides, which emit a gamma ray almost simultaneously with the positron, are used as positron sources in lifetime measurement studies[6]. The widely used Na^{22} source emits a 1.28-MeV photon within 3 ps of the emission of the preceding positron. The detection of the gamma ray marks the zero time (reference time) for a lifetime measurement since the thermalization time for the positrons in condensed matter is very short. Typical lifetime spectra in polymers are shown in figures 9(a) and 9(b).

PAS has been used extensively in the study of metals, glasses, and polymers. It has been used to monitor the physical state of metals, their defect concentration, and fatigue damage. Because positrons annihilate mostly in localized sites—such as defects or vacancies—their annihilation characteristics reflect the electronic structure of defects. For example, as a result of PAS studies, it is now known that a vacancy is not just an empty hole in the lattice but has an electron density at its center equal to about a third of the bulk electron density (ref. 59). The electron density inside the voids, however, quickly approaches zero as the void size increases. Perhaps the keenest interest in PAS has been exhibited by the polymer scientists. They have used it extensively for characterizing polymers (refs. 60 to 66), including studies of glass transition temperatures, free volume, effects of metal ions on polymer chemical architecture, and the effects of chemical additives and processing techniques on polymer physical properties.

More detailed discussions of positron annihilation and related phenomena in solids can be found in references 67 to 69.

Synchrotron radiation. Whenever charged particles experience acceleration (such as when they move along a circular path), they radiate energy as

dilute nonmagnetic impurities in iron alloys. For example, the average fractional change per unit concentration of Al impurity in the hyperfine field at the Fe site in Fe(Al) because of the neighboring Al atoms has been reported (refs. 25 to 27) to be of the order of -0.4 to -0.5 by Mössbauer measurements as opposed to $-0.35 + 0.03$ by μSR measurements (ref. 48). Both these measurements support the conclusion that the change results from changes in conduction electron polarization and spin-density fluctuations.

[6] Recent attempts (ref. 58) at accelerator-produced positron sources depend on $\beta^+\gamma$ coincidence systems where the Cerenkov signal by the positrons themselves provides the time marker signal.

predicted by Maxwell's equations. At low energies, the particles emit radiation primarily at their frequency of revolution. At higher energies, the spectrum acquires higher order harmonics of the particle revolution frequency. For a particle of energy E, the radiated spectrum extends from the frequency of revolution ω to $\gamma^3\omega$, where $\gamma = \frac{1}{(1-v^2/c^2)^{1/2}}$ (refs. 70 and 71). Since this radiated energy was first recognized by the nuclear physicists as the basic limitation on the energy attainable with an electron synchrotron, it is called synchrotron radiation (SR). Because of lack of precision of orbital frequency in practical accelerators, the synchrotron radiation spectrum $P(\lambda)$ (refs. 70 to 74) is a continuum given by the following expression:

$$P(\lambda) = \frac{e^{5/2}}{16\pi^2}\frac{e^2 c}{R^3}\left(\frac{E}{m_0 c^2}\right)^7 G\left(\frac{\lambda}{\lambda_p}\right) \qquad (11)$$

where R is the radius of curvature of the path of a particle of mass m_0, λ_p is the wavelength at the peak of the radiated power spectrum, and $G\left(\frac{\lambda}{\lambda_p}\right)$ is the power spectrum function, given analytically in terms of integrals of modified Bessel functions. Since the radiating particles in all existing synchrotron facilities are electrons, equation (11) can be modified as follows (ref. 72):

$$P(\lambda) = 0.9\left(\frac{E^7}{R^3}\right) G\left(\frac{\lambda}{\lambda_p}\right) \qquad (12)$$

where $\lambda_p = 2.35\frac{R}{E^3}$. Rewriting equation (12) in terms of number of photons radiated per second per unit wavelength and per unit solid angle, we have (ref. 72)

$$\frac{dI}{d\lambda} = (7.86)10^{11}\, J\frac{\lambda}{\lambda_c}\frac{E^7}{R^2}G\left(\frac{\lambda}{\lambda_p}\right) \qquad (13)$$

where J is the average particle current in milliamps and λ_c is the critical wavelength in angstroms. (The term λ_c is a measure of the lower limit of the wavelength distribution and is equal to $2.38\lambda_p$.) Integrating the power loss over all wavelengths and over all angles, we can write the loss in energy δE suffered by an orbiting particle of energy E as follows (ref. 72):

$$\delta E = 88.5\frac{E^4}{R} \qquad (14)$$

Clearly δE is a very strong function of electron energy E and the local radius of curvature R of its path. Quite often, the spectral properties of SR from an electron accelerator can be changed by locally changing the R value. Synchrotron radiation from highly relativistic particles is strongly polarized in the plane of its orbit. The spectrum is also a function of the angle of elevation ϕ with respect to the plane of orbit of the electrons, with shorter wavelengths more highly concentrated in the $\phi = 0°$ direction (refs. 70 to 74).

Although the SR limits the energies attainable with circular electron accelerators and storage rings, it also provides access to a highly useful region of the electromagnetic spectrum extending from 1000 Å down to 0.1 Å. The continuously selectable intense beams of SR are being used to explore the outer and inner electronic structure of solids. By measuring small- and wide-angle scattering of SR during crystallization and solid-state phase transitions in polymers, very useful information about polymers in the solid-state phase can be obtained (ref. 75).

One intriguing application of SR concerns possible excitation of Mössbauer states (refs. 76 and 77), particularly in those nuclei where conventional techniques cannot work or where special characteristics of SR suggest new, interesting possibilities. However, typical fluxes of photons in the energy range of intrinsic widths of the most commonly used Mössbauer nuclei amount to only about 10^{-14} to 10^{-13} of the gross beam. Clearly, this calls for a special monochromatization in order to enhance the resonant quanta flux in the beam at the Mössbauer target.

A significant technological application of SR concerns the development of microminiaturized integrated circuits. Through use of SR at 20 Å, the resolution of the circuit pattern can be reduced to about 100 Å, an improvement by a factor of 100 over the visible wavelength. Synchrotron X-ray fluorescence (SXRF) complements conventional X-ray fluorescence (XRF) in elemental analysis of solids. It can provide capabilities with minimum detection limits of less than 1 ppm for 20-μm-beam spots (ref. 78). A more recent application of synchrotron radiation involves three-dimensional microtomography of small material samples reported by Flannery et al. (ref. 79). This new technique nondestructively generates three-dimensional maps of density and elemental distributions in the samples with a spatial resolution of the order of 1 μm and an accuracy of approximately 1 percent. Another SR application of great current interest involves high-resolution studies for the high-temperature superconductors (refs. 80 and 81). More detailed discussions of synchrotron radiation and its applications in solids can be found in references 82 to 86.

Concluding Remarks

Nuclear techniques have played an important role in the studies of materials over the past several

decades. Earlier applications were confined largely to the technological and environmental problems. For example, neutron radiography and neutron diffraction techniques were used for the investigation of structural defects and stress-induced changes in metals and metal compounds. Later on, neutron activation, charged-particle activation, X-ray-induced fluorescence, and charged-particles-induced X-ray emission techniques were used extensively for the analysis of industrial and environmental samples. Some of the more recent developments in nuclear physics have opened up several fields where nuclear techniques can help solve outstanding problems. Four such techniques—Mössbauer spectrocopy (MS), muon spin rotation (μ^+SR), positron annihilation spectroscopy (PAS), and synchrotron radiation (SR)—have been reviewed and some of their current applications identified. Mössbauer spectroscopy is finding extensive applications in solid-state physics, chemistry, and biology. The extreme sensitivity of the Mössbauer parameters to the electronic structure of the Mössbauer nuclide and its neighbors has helped resolve some major problems in high-stress structures, hydrogen embrittlement in steels, and the theory of spin glasses. From an atomic viewpoint, a positive muon can be looked upon as a light isotope of hydrogen. Muon spin rotation is thus a rather sensitive probe for hydrogen in metals study. Like MS, μ^+SR is very sensitive to the electronic structure of the host and impurity atoms in the test object. Positrons, like MS and μ^+SR, are also very sensitive to the electronic structure and configuration of the test material. In most nonconductors, particularly polymers, they form positronium atoms whose subsequent annihilation provides very useful information about the defect structure of the test objects. Synchrotron radiation has filled a very useful gap in the available electromagnetic spectrum for atomic-molecular and solid-state studies. An application of SR that is being eagerly pursued is the spectroscopy of solids. Both the band structure of the outer electrons and the once-inaccessible higher energy spectrum of the core electrons are now being explored with the synchrotron radiation. All these techniques are proving to be very useful in the characterization of structures. It is hoped that their intensified applications will lead to the development of new and improved materials.

NASA Langley Research Center
Hampton, VA 23665-5225
October 23, 1987

References

1. Mistry, V. D.; Hollas, C. L.; Hiddleston, H. R.; and Riley, P. J.: Isobaric Analog Resonances in Proton Elastic Scattering From ^{110}Cd, ^{112}Cd, and ^{114}Cd. *Nuclear Isospin,* John D. Anderson, Stewart D. Bloom, Joseph Cerny, and William W. True, eds., Academic Press, 1969, pp. 673–678.
2. Enge, Harald A.: *Introduction to Nuclear Physics.* Addison-Wesley Publ. Co., Inc., c.1966.
3. Singh, Jag J.: Measurement of Trace Metals in Coal Plant Effluents—A Review. *Environmental and Climatic Impact of Coal Utilization,* Jag J. Singh and Adarsh Deepak, eds., Academic Press, Inc., 1980, pp. 101–132.
4. Chu, Wei-Kan; Mayer, James W.; and Nicolet, Marc-A.: *Backscattering Spectrometry.* Academic Press, Inc., 1978.
5. Magee, Charles W.; and Hewitt, Lori R.: Rutherford Backscattering Spectrometry: A Quantitative Technique for Chemical and Structural Analysis of Surfaces and Thin Films. *RCA Rev.,* vol. 47, no. 2, June 1986, pp. 162–185.
6. Johansson, Sven A. E.; and Johansson, Thomas B.: Analytical Application of Particle Induced X-Ray Emission. *Nucl. Instrum. & Methods,* vol. 137, no. 3, Sept. 1976, pp. 473–516.
7. Cahill, T. A.: Proton Microprobes and Particle-Induced X-Ray Analytical Systems. *Annual Review of Nuclear and Particle Science, Volume 30,* J. D. Jackson, Harry E. Gove, and Roy F. Schwitters, eds., Annual Reviews Inc., 1980, pp. 211–252.
8. Campbell, J. L.; and Cookson, J. A.: PIXE Analysis of Thick Targets. *Nucl. Instrum. & Methods Phys. Res.,* vol. 231 (B3), no. 1-3, Apr.–May 1984, pp. 185–197.
9. Lanford, W. A.; Trautvetter, H. P.; Ziegler, J. F.; and Keller, J.: New Precision Technique for Measuring the Concentration Versus Depth of Hydrogen in Solids. *Appl. Phys. Lett.,* vol. 28, no. 9, May 1, 1976, pp. 566–568.
10. Doyle, B. L.; and Peercy, P. S.: Technique for Profiling ^{1}H With 2.5-MeV Van de Graaff Accelerators. *Appl. Phys. Lett.,* vol. 34, no. 11, June 1, 1979, pp. 811–813.
11. Lanford, William A.: Analysis With Heavy Ions. *Treatise on Heavy-Ion Science, Volume 6—Astrophysics, Chemistry, and Condensed Matter,* D. Allan Bromley, ed., Plenum Press, c.1985, pp. 363–394.
12. Wielunski, L. S.; Benenson, R. E.; and Lanford, W. A.: Helium-Induced Hydrogen Recoil Analysis for Metallurgical Applications. *Nucl. Instrum. & Methods Phys. Res.,* vol. 218, nos. 1–3, Dec. 15, 1983, pp. 120–124.
13. Amsel, G.; and Lanford, W. A.: Nuclear Reaction Techniques in Materials Analysis. *Annual Review of Nuclear and Particle Science, Volume 34,* J. D. Jackson, Harry E. Gove, and Roy F. Schwitters, eds., Annual Reviews Inc., 1984, pp. 435–460.
14. Xiong, Fulin; Rauch, F.; Shi, Chengru; Zhou, Zhuying; Livi, R. P.; and Tombrello, T. A.: Hydrogen Depth Profiling in Solids: A Comparison of Several Resonant Nuclear Reaction Techniques. *Nucl. Instrum. & Methods Phys. Res.,* vol. B27, no. 3, July 1, 1987, pp. 432–441.
15. Fatemi, M.; Pande, C. S.; and Rath, B. B.: Applications of Small-Angle Neutron Scattering Method (SANS) in Non-Destructive Evaluation (NDE). *Novel NDE Methods*

for Materials, Bhakta B. Rath, ed., American Inst. of Mining, Metallurgical, and Petroleum Engineers, Inc., c.1983, pp. 155–191.

16. Axe, John D.; and Nicklow, Robert M.: Neutron Scattering in Condensed-Matter Physics. *Phys. Today,* vol. 38, no. 1, Jan. 1985, pp. 27–35.
17. Stein, Richard S.; and Han, Charles C.: Neutron Scattering From Polymers. *Phys. Today,* vol. 38, no. 1, Jan. 1985, pp. 74–80.
18. *Report of the Review Panel on Neutron Scattering.* IS-4761 (Contract W-7406-eng-82), Ames Lab., Iowa State Univ., Oct. 22, 1980.
19. Robinson, Arthur L.: An Oxygen Key to the New Superconductors. *Science,* vol. 236, no. 4805, May 29, 1987, pp. 1063–1065.
20. Moon, Ralph M.: Slow Neutron Scattering Experiments. *Science,* vol. 230, no. 4723, Oct. 18, 1985, pp. 274–280.
21. Schmank, M. J.; and Krawitz, A. D.: Measurement of a Stress Gradient Through the Bulk of an Aluminum Alloy Using Neutrons. *Metall. Trans.,* vol. 13A, no. 6, June 1982, pp. 1069–1076.
22. Wertheim, Gunther K.: Mössbauer Effect: *Principles and Applications.* Academic Press, Inc., c.1964.
23. May, Leopold, ed.: *An Introduction to Mössbauer Spectroscopy.* Plenum Press, 1971.
24. Van Rossum, M.: Characterization of Solids by Mössbauer Spectroscopy. *Prog. Cryst. Growth & Charact.,* vol. 5, no. 1/2, 1982, pp. 1–45.
25. Singh, Jag J.: *Mössbauer Effect in Dilute Iron Alloys.* NASA TM X-72810, 1975.
26. Singh, Jag J.: *Mössbauer Effect Studies in Iron Containing Nonmagnetic Impurities.* NASA TM-74067, 1977.
27. Singh, Jag J.: Mössbauer Effect Measurement in Single Crystal Iron Subjected to Cyclic Stress. *Nucl. Instrum. & Methods,* vol. 134, no. 2, Apr. 15, 1976, pp. 363–368.
28. Hafemeister, David W.: Nuclear Properties Determined From Mössbauer Measurements. *An Introduction to Mössbauer Spectroscopy,* Leopold May, ed., Plenum Press, 1971, pp. 45–74.
29. Michaelsen, C.; and Hellstern, E.: Mössbauer Effect on Mechanically Alloyed Fe-Zr Glasses. *J. Appl. Phys.,* vol. 62, no. 1, July 1, 1987, pp. 117–119.
30. Schiess, James R.; and Singh, Jag J.: *A Computer Program for Analyzing Unresolved Mössbauer Hyperfine Spectra.* NASA TM-78633, 1978.
31. Fujita, F. E.: Mössbauer Effect Study of the Structure and Structural Units in Amorphous Alloys. *At. Energy Rev.,* suppl. no. 1, 1981, pp. 173–202.
32. Gonser, U.: Mössbauer Spectroscopy on Amorphous Metals. *At. Energy Rev.,* suppl. no. 1, 1981, pp. 203–228.
33. Berry, Frank J.: Mössbauer Spectroscopy. *Phys. Bull.,* vol. 34, no. 12, Dec. 1983, pp. 517–519.
34. Campbell, S. J.: An Introduction to Mössbauer Studies of Magnetic Materials. *Australian J. Phys.,* vol. 37, no. 4, 1984, pp. 429–447.
35. Gonser, U., ed.: *Mössbauer Spectroscopy.* Springer-Verlag, 1975.
36. Stevens, John G.; and Shenoy, Gopal K., eds.: *Mössbauer Spectroscopy and Its Chemical Applications.* American Chemical Soc., 1981.
37. Eibschutz, M.; Murphy, D. W.; Sunshine, S.; Van Uitert, L. G.; Zahurak, S. M.; and Grodkiewicz, W. H.: Electronic Structure of Eu in the High-T_c Superconductor $Ba_2EuCu_3O_{7-1}$. *Phys. Rev. B,* vol. 35, no. 16, June 1, 1987, pp. 8714–8715.
38. Longworth, Geoffrey: The Use of Mössbauer Spectroscopy in Materials Science. *Treatise on Materials Science and Technology, Volume 19—Experimental Methods, Part A,* Herbert Herman, ed., Academic Press, Inc., 1980, pp. 107–150.
39. Kalvius, G. M.: Mössbauer Spectroscopy of Actinides: Some Applications to Solid State Chemistry. *J. Less-Common Met.,* vol. 121, 1986, pp. 353–378.
40. Schenck, A.: *Muon Spin Rotation Spectroscopy—Principles and Applications in Solid State Physics.* Adam Hilger Ltd., c.1985.
41. Fleming, Donald G.; Garner, David M.; Vaz, Louis C.; Walker, David C.; Brewer, Jesse H.; and Crowe, Kenneth M.: Muonium Chemistry—A Review. *Positronium and Muonium Chemistry,* Hans J. Ache, ed., American Chemical Soc., 1979, pp. 279–334.
42. Abragam, A.: *The Principles of Nuclear Magnetism.* Clarendon Press (Oxford), 1961.
43. Gurevich, I. I.; Meléshko, E. A.; Muratova, I. A.; Nikolśky, B. A.; Roganov, V. S.; Selivanov, V. I.; and Sokolov, B. V.: Dipole Interactions and Diffusion of μ^+ Meson in Copper. *Phys. Lett.,* vol. 40A, no. 2, July 3, 1972, pp. 143–144.
44. Brewer, J. H.; Crowe, K. M.; Gygax, F. N.; and Schenck, A.: Positive Muons and Muonium in Matter. *Muon Physics, Volume III—Chemistry,* Vernon W. Hughes and C. S. Wu, eds., Academic Press, Inc., 1975, pp. 3–139.
45. Yamazaki, T.: Muon Spin Relaxation in Magnetic Materials. *Hyperfine Interact.,* vol. 6, no. 1–4, Jan.–Feb. 1979, pp. 115–125.
46. Hayano, R. S.; Uemura, Y. J.; Imazato, J.; Nishida, N.; Yamazaki, T.; and Kubo, R.: Zero- and Low-Field Spin Relaxation Studied by Positive Muons. *Phys. Rev. B.,* vol. 20, no. 3, Aug. 1, 1979, pp. 850–859.
47. Lankford, William F.; Lynn, Kelvin G.; Kossler, William J.; Fiory, Anthony T.; Minnich, R. Paul; and Stronach, Carey E.: Current Techniques in Muon Spin Rotation Experiments. *Nucl. Instrum. & Methods,* vol. 185, no. 1–3, June 1981, pp. 469–480.
48. Stronach, C. E.; Kossler, W. J.; Lindemuth, J.; Petzinger, K. G.; Fiory, A. T.; Minnich, R. P.; Lankford, W. F.; Singh, J. J.; and Lynn, K. G.: Muon Hyperfine Fields in Fe(Al) Alloys. *Phys. Rev. B,* vol. 20, no. 6, Sept. 15, 1979, pp. 2315–2322.
49. Edwards, S. F.; and Anderson, P. W.: Theory of Spin Glasses: II. *J. Phys. F: Metal Phys.,* vol. 6, no. 10, Oct. 1976, pp. 1927–1937.
50. Murnick, D. E.; Fiory, A. T.; and Kossler, W. J.: Muon-Spin Depolarization in Spin-Glasses. *Phys. Rev. Lett.,* vol. 36, no. 2, Jan. 12, 1976, pp. 100–104.
51. Schenck, Alexander: The Electronic Structure of Hydrogen in Elemental Metals in the Light of Muon Spin Rotation (μSR) Investigations. *Helvetica Physica Acta,* vol. 54, no. 4, 1981, pp. 471–546.

52. Kossler, W. J.; Kempton, J. R.; Yu, X. H.; Schone, H. E.; Uemura, Y. J.; Moodenbaugh, A. R.; Suenaga, M.; and Stronach, C. E.: Magnetic Field Penetration Depth of $La_{1.85}Sr_{0.15}CuO_4$ Measured by Muon Spin Relaxation. *Phys. Rev. B.*, vol. 35, no. 13, May 1, 1987, pp. 7133–7136.
53. Uemura, Y. J.; Kossler, W. J.; Yu, X. H.; Kempton, J. R.; Schone, H. E.; Opie, D.; Stronach, C. E.; Johnston, D. C.; Alvarez, M. S.; and Goshorn, D. P.: Antiferromagnetism of La_2CuO_{4-y} Studied by Muon-Spin Rotation. *Phys. Rev. Lett.*, vol. 59, no. 9, Aug. 31, 1987, pp. 1045–1048.
54. Aeppli, G.; Cava, R. J.; Ansaldo, E. J.; Brewer, J. H.; Kreitzman, S. R.; Luke, G. M.; Noakes, D. R.; and Kiefl, R. F.: Magnetic Penetration Depth and Flux-Pinning Effects in High-T_c Superconductor $La_{1.85}Sr_{0.15}CuO_4$. *Phys. Rev. B,* vol. 35, no. 13, May 1, 1987, pp. 7129–7132.
55. Harshman, D. R.; Aeppli, G.; Ansaldo, E. J.; Batlogg, B.; Brewer, J. H.; Carolan, J. F.; Cava, R. J.; Celio, M.; Chaklader, A. C. D.; Hardy, W. N.; Kreitzman, S. R.; Luke, G. M.; Noakes, D. R.; and Senba, M.: Temperature Dependence of the Magnetic Penetration Depth in the High-T_c Superconductor $Ba_2YCu_3O_{9-\delta}$: Evidence for Conventional s-Wave Pairing. *Phys. Rev. B,* vol. 36, no. 4, Aug. 1, 1987, pp. 2386–2389.
56. Fiory, A. T.; Murnick, D. E.; Leventhal, M.; and Kossler, W. J.: Probing the Superconducting Vortex Structure by Polarized-μ^+ Spin Precession. *Phys. Rev. Lett.*, vol. 33, no. 16, Oct. 14, 1974, pp. 969–972.
57. Gladisch, M.; Orth, H.; Putlitz, G. Zu; Wahl, W.; Wigand, M.; Herlach, D.; Metz, H.; Seeger, A.; and Teichler, H.: Muon Spin Rotation in Superconductors. *Hyperfine Interact.*, vol. 6, no. 1–4, Jan–Feb. 1979, pp. 109–112.
58. Bauer, W.; Maier, K.; Major, J.; Schaefer, H.-E.; Seeger, A.; Carstanjen, H.-D.; Decker, W.; Diehl, J.; and Stoll, H.: The Positron Beam at the Stuttgart Pelletron Accelerator and Its Applications to $\beta^+\gamma$ Positron Lifetime Measurements. *Appl. Phys. A,* vol. 43, no. 4, Aug. 1987, pp. 261–267.
59. Manninen, M.; Nieminen, R.; Hautojärvi, P.; and Arponen, J.: Electrons and Positrons in Metal Vacancies. *Phys. Rev. B,* vol. 12, no. 10, Nov. 15, 1975, pp. 4012–4022.
60. Hamielec, A. E.; Eldrup, M.; Mogensen, O.; and Jansen, P.: Positron Annihilation Techniques (PAT) in Polymer Science and Engineering. *Reviews in Macromolecular Chemistry, Volume 10,* George B. Butler, Kenneth F. O'Driscoll, and Mitchel Shen, eds., Marcel Dekker, Inc., 1973, pp. 305–337.
61. Singh, Jag J.; St. Clair, Terry L.; Holt, William H.; and Mock, Willis, Jr.: Moisture Dependence of Positron Annihilation Spectra in Nylon-6. *Nucl. Instrum. & Methods Phys. Res.*, vol. 221, no. 2, Apr. 1, 1984, pp. 427–432.
62. Singh, Jag J.; and Stoakley, Diane M.: *Investigation of the Effects of Cobalt Ions on Epoxy Properties.* NASA TP-2639, 1986.
63. Singh, Jag J.; Stoakley, Diane M.; Holt, William H.; Mock, Willis M., Jr.; and Teter, Joseph P.: Effects of Transition Metal Ions on Positron Annihilation Characteristics in Epoxies. *Nucl. Instrum. & Methods Phys. Res.*, vol. B26, no. 4, June 1987, pp. 598–602.
64. Jean, Y. C.; Sandreczki, T. C.; and Ames, D. P.: Positronium Annihilation in Amine-Cured Epoxy Polymers. *J. Polymer Phys.*, vol. 24, no. 6, pt. B, 1986, pp. 1247–1258.
65. Sandreczki, T. C.; Brown, I. M.; Jean, Y. C.; and Wang, Y. Y.: Separation of Free Volume and Temperature Effects on Molecular Mobility in Cured Epoxy Resins. *Polymer Mater. Sci. & Eng.*, vol. 55, 1986, pp. 69–71.
66. Stevens, J. R.: Positron Annihilation. *Polymers—Part A: Molecular Structure and Dynamics,* R. A. Fava, ed., Volume 16 of Methods of Experimental Physics, Academic Press, Inc., 1980, pp. 371–403.
67. Hautojärvi, P., ed.: *Positrons in Solids.* Springer-Verlag, 1979.
68. Brandt, W.; and Dupasquier, A., eds.: Proceedings of the International School of Physics "Enrico Fermi"—Course LXXXIII, *Positron Solid-State Physics.* North-Holland Publ. Co., 1983.
69. Mills, Allen P., Jr.: Surface Analysis and Atomic Physics With Slow Positron Beams. *Science,* vol. 218, no. 4570, Oct. 22, 1982, pp. 335-340.
70. Koch, Ernst-Eckhard; Eastman, Dean Eric; and Farge, Yves: Synchrotron Radiation—A Powerful Tool in Science. *Handbook on Synchrotron Radiation, Volume 1A,* Ernst-Eckard Koch, ed., North-Holland Publ. Co., 1983, pp. 1–63.
71. Krinsky, S.; Perlman, M. L.; and Watson, R. E.: Characteristics of Synchrotron Radiation and of Its Sources. *Handbook on Synchrotron Radiation, Volume 1A,* Ernst-Eckhard Koch, ed., North-Holland Publ. Co., 1983, pp. 65–171.
72. Rowe, Ednor M.: Synchrotron Radiation—Facilities in the United States. *Phys. Today,* vol. 34, no. 5, May 1981, pp. 28–32, 34–37.
73. Sparks, Cullie J., Jr.: Synchrotron Radiation—Research With X rays. *Phys. Today,* vol. 34, no. 5, May 1981, pp. 40–49.
74. Doniach, Seb; and Winick, Herman, eds.: *Synchrotron Radiation Research.* Plenum Press, 1980.
75. Elsner, Gerhard; Riekel, Christian; and Zachmann, Hans Gerhard: Synchrotron Radiation in Polymer Science. *Characterization of Polymers in the Solid State II: Synchrotron Radiation, X-Ray Scattering and Electron Microscopy,* H. H. Kausch and H. G. Zachmann, eds., Springer-Verlag, c.1985, pp. 1–57.
76. Artemyev, A. N.; Kabannik, V. A.; Kazakov, Yu. N.; Kulipanov, G. N.; Meleshko, E. A.; Sklyarevskiy, V. V.; Skrinsky, A. N.; Stepanov, E. P.; Khlestov, V. B.; and Chechin, A. I.: Utilization of the Specific Characteristics of the Synchrotron Radiation in Experiments of the ^{57m}Fe Mössbauer Level Excitation. *Nucl. Instrum. & Methods,* vol. 152, no. 1, June 1, 1978, pp. 235–241.
77. Cohen, R. L.: Nuclear Resonance Experiments Using Synchrotron Radiation Sources. *Synchrotron Radiation*

Research., Seb Doniach and Herman Winick, eds., Plenum Press, 1980, pp. 647–662.

78. Sutton, S. R.; Rivers, M. L.; and Smith, J. V.: Applications of Synchrotron X-Ray Fluorescence to Extraterrestrial Materials. *Nucl. Instrum. & Methods Phys. Res.*, vol. B24/25, pt. 1, Apr. 1987, pp. 405–409.
79. Flannery, Brian P.; Deckman, Harry W.; Roberge, Wayne G.; and D'Amico, Kevin L.: Three-Dimensional X-ray Microtomography. *Science,* vol. 237, no. 4821, Sept. 18, 1987, pp. 1439–1444.
80. Moss, S. C.; Forster, K.; Axe, J. D.; You, H.; Hohlwein, D.; Cox, D. E.; Hor, P. H.; Meng, R. L.; and Chu, C. W.: High-Resolution Synchrotron X-Ray Study of the Structure of $La_{1.8}BA_{0.2}CuO_{4-y}$. *Phys. Rev. B,* vol. 35, no. 13, May 1, 1987, pp. 7195–7198.
81. Qadri, S. B.; Toth, L. E.; Osofsky, M.; Lawrence, S.; Gubser, D. U.; and Wolf, S. A.: X-Ray Identification of the Superconducting High-T_c Phase in the Y-Ba-Cu-O System. *Phys. Rev. B.*, vol. 35, no. 13, May 1, 1987, pp. 7235–7237.
82. Kunz, C., ed.: *Synchrotron Radiation—Techniques and Applications.* Springer-Verlag, 1979.
83. Howells, Malcolm R., ed.: *Reflecting Optics for Synchrotron Radiation.* Volume 315 of Proceedings of SPIE—The International Society for Optical Engineering. Soc. of Photo-Optical Instrumentation Engineers, c.1982.
84. Koch, Ernst-Eckhard, ed.: *Handbook on Synchrotron Radiation, Volume 1B* North-Holland Publ. Co., 1983.
85. Blume, Martin; and Moncton, David E.: Large Facilities for Condensed-Matter Science. *Phys. Today,* vol. 38, no. 3, Mar. 1985, pp. 68–76.
86. Kausch, H. H.; and Zachmann, H. G., eds.: *Characterization of Polymers in the Solid State II. Synchrotron Radiation, X-ray Scattering and Electron Microscopy.* Springer-Verlag, c.1985.

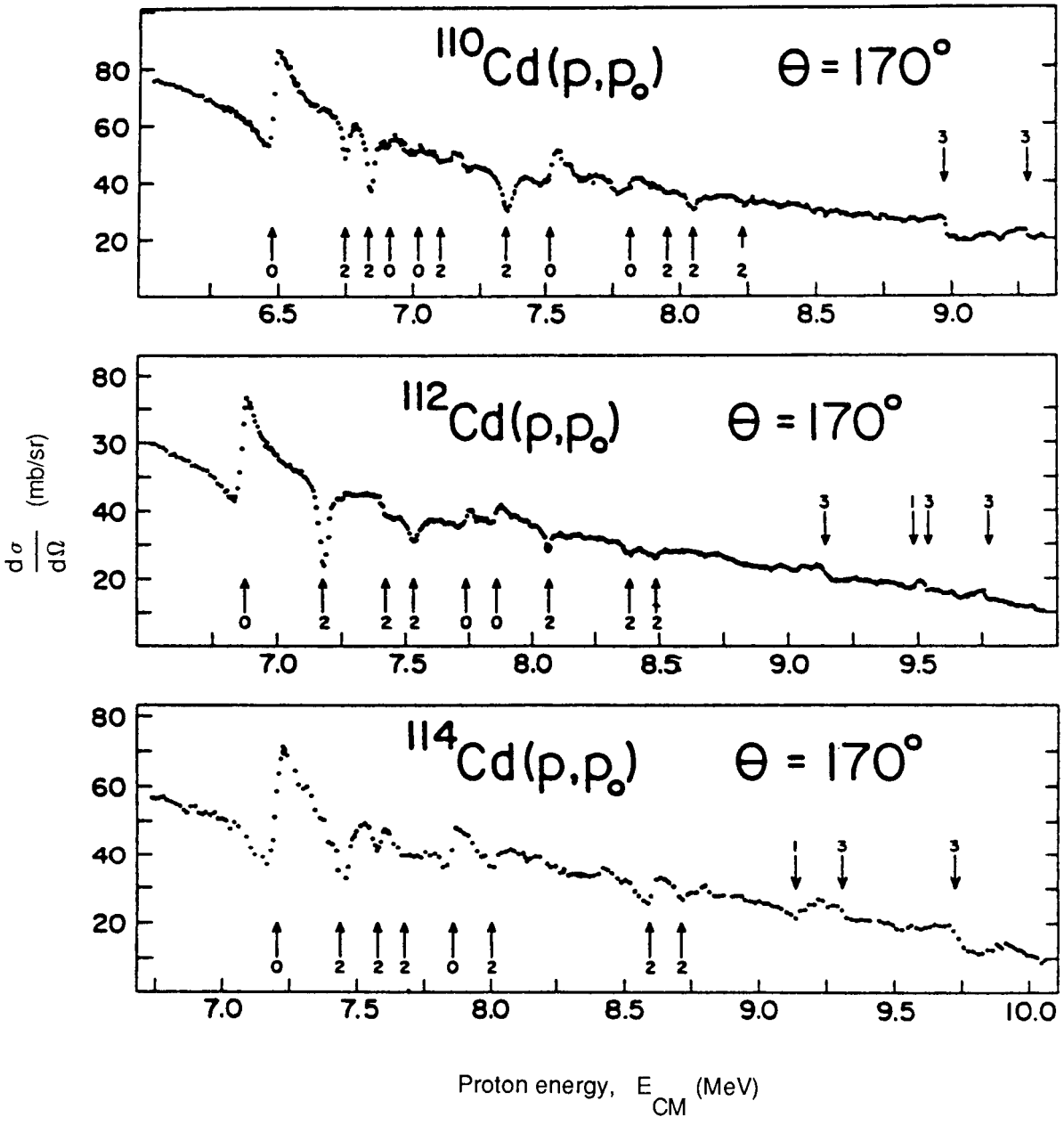

Figure 1. Excitation functions for three Cd isotopes at laboratory angle of 170°. (From ref. 1.)

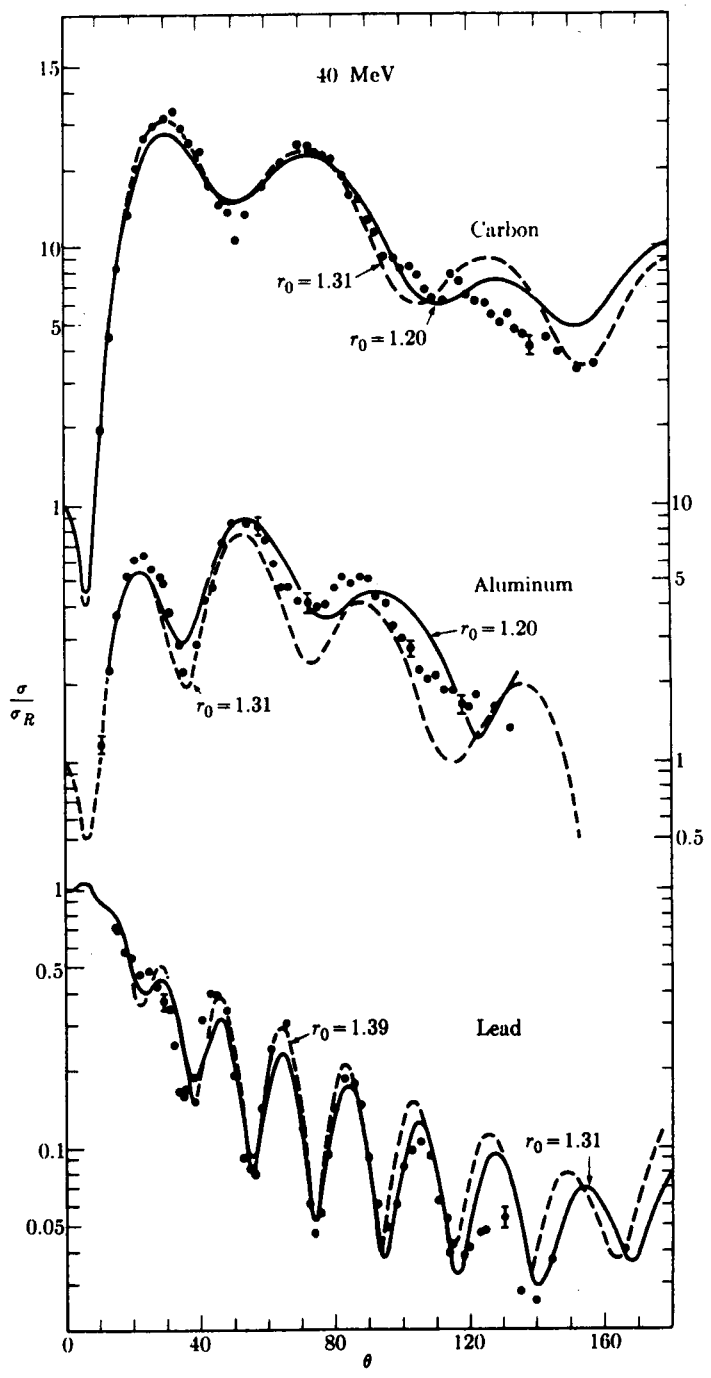

Figure 2. Elastic scattering cross sections for 40-MeV protons on various targets. (From ref. 2.)

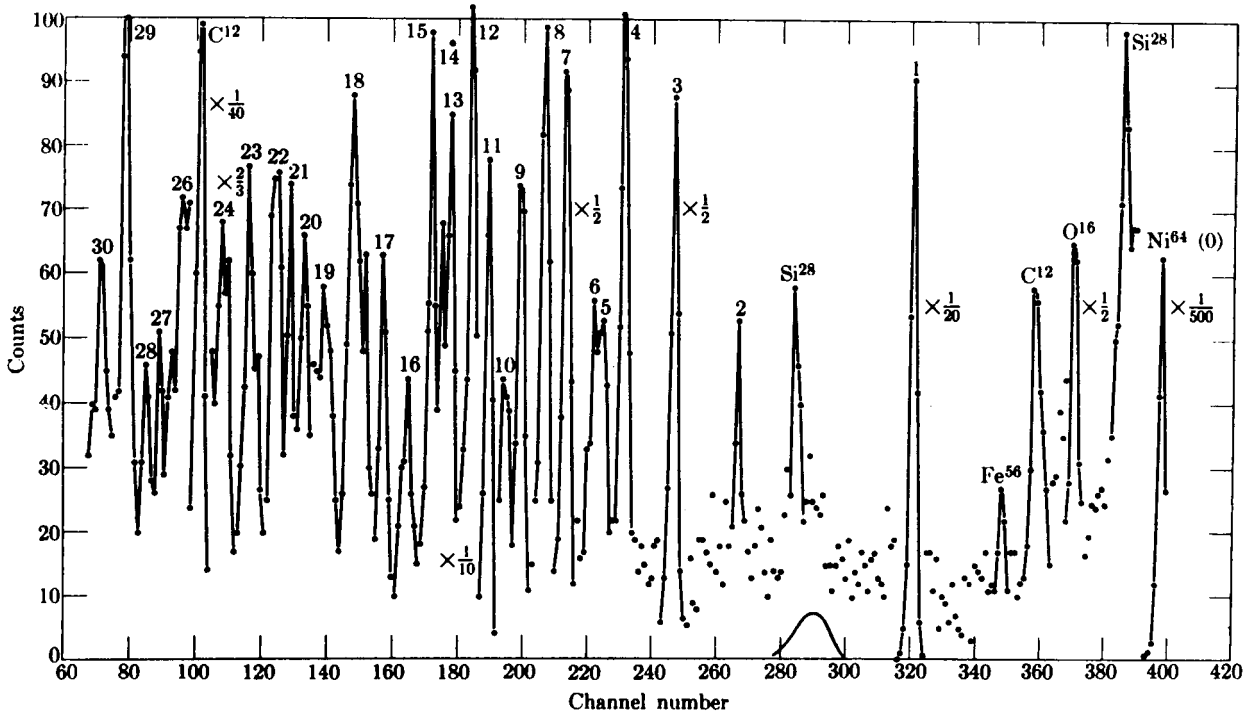

Figure 3. Pulse-height spectrum of protons elastically and inelastically scattered from a thin (1 mg/cm^2) Ni^{64} target. Incident proton energy $T_I = 11$ MeV; reaction angle $\theta = 60°$. (From ref. 2.)

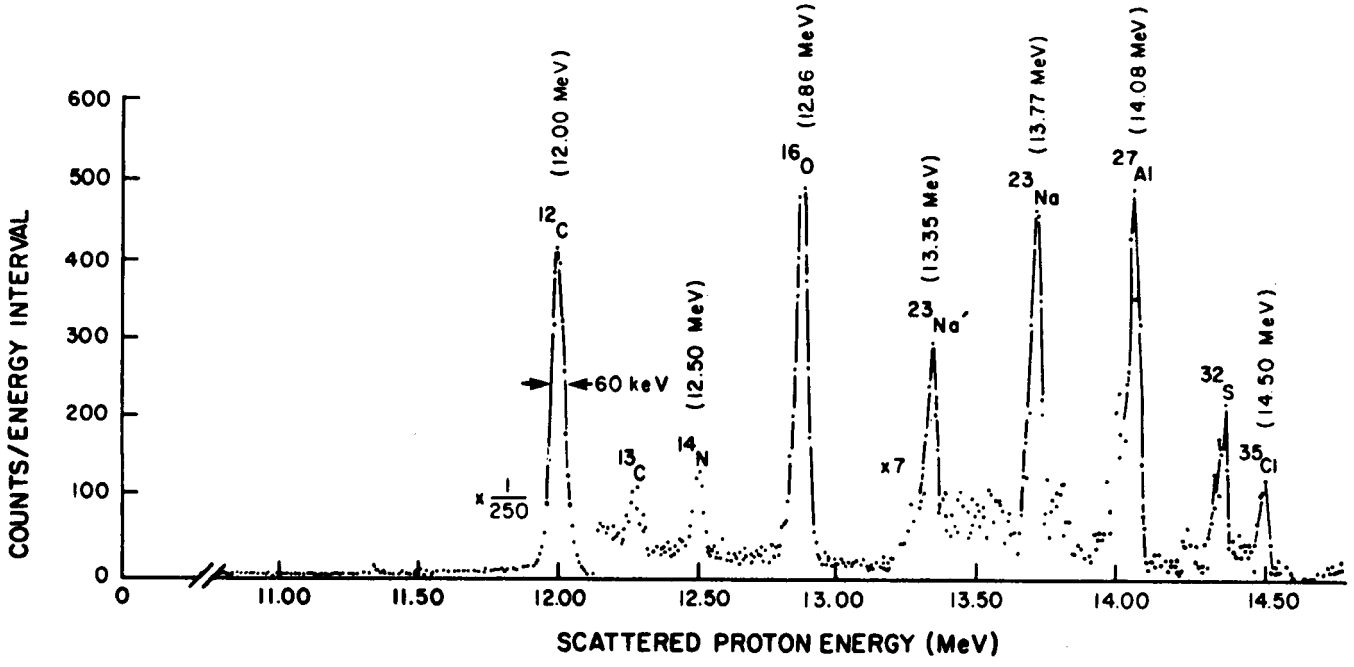

Figure 4. Spectrum of 16 MeV protons scattered from aerosol sample at $\theta_{Lab} = 135°$. $Q = 4\ \mu C$. (From ref. 3.)

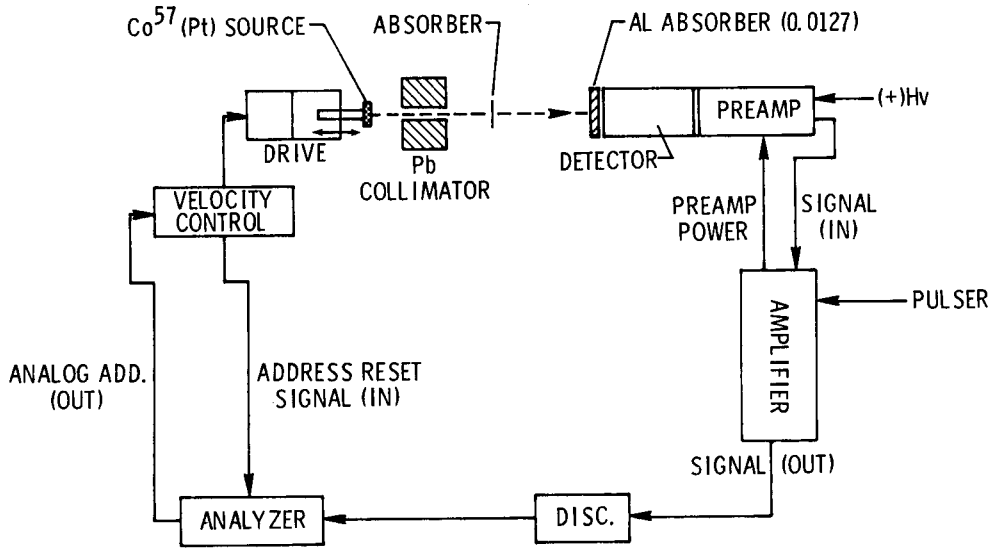

(a) Transmission geometry.

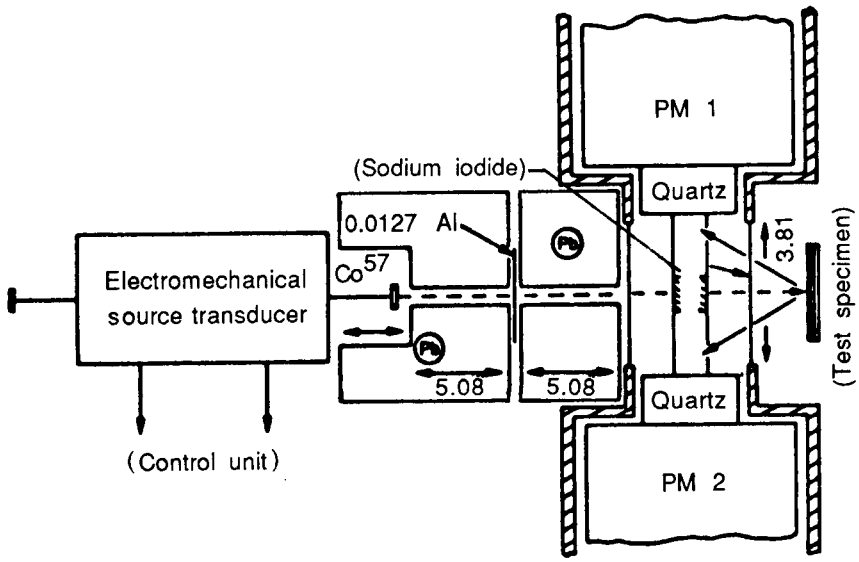

(b) Backscattering geometry. Dimensions in centimeters.

Figure 5. Block diagrams of Mössbauer spectrometer. Dimensions in centimeters.

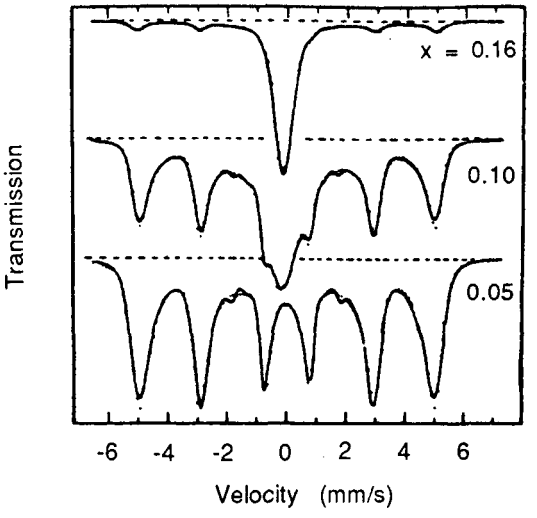

(a) Mössbauer spectra of iron-rich, mechanically alloyed $Fe_{1-x}Zr_x$ recorded at room temperature. (From ref. 29.)

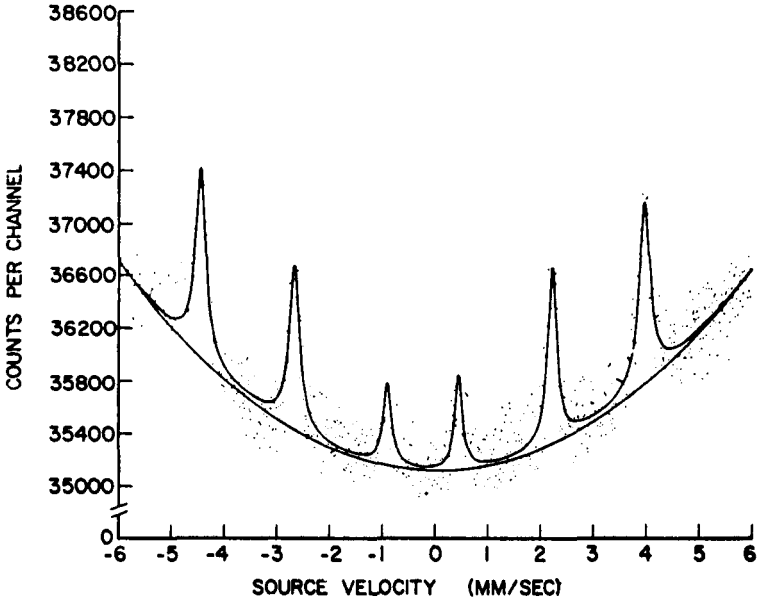

(b) Typical backscattered Mössbauer spectrum obtained from single-crystal iron specimen subjected to 600×10^3 fatigue cycles in the stress range of 3 to 7 kg/mm^2. (From refs. 25 to 27.)

Figure 6. Typical Mössbauer spectra in iron and iron alloys.

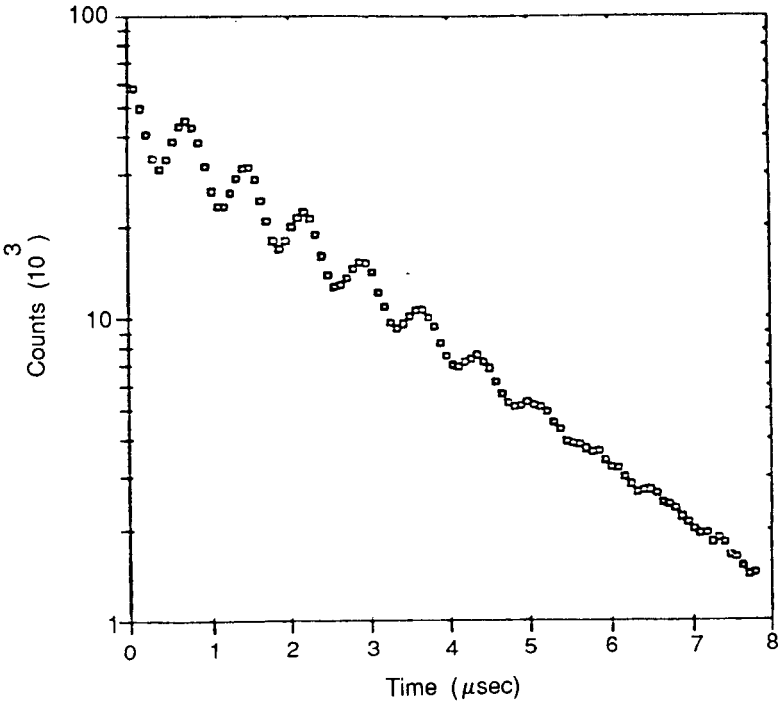

(a) Iron target.

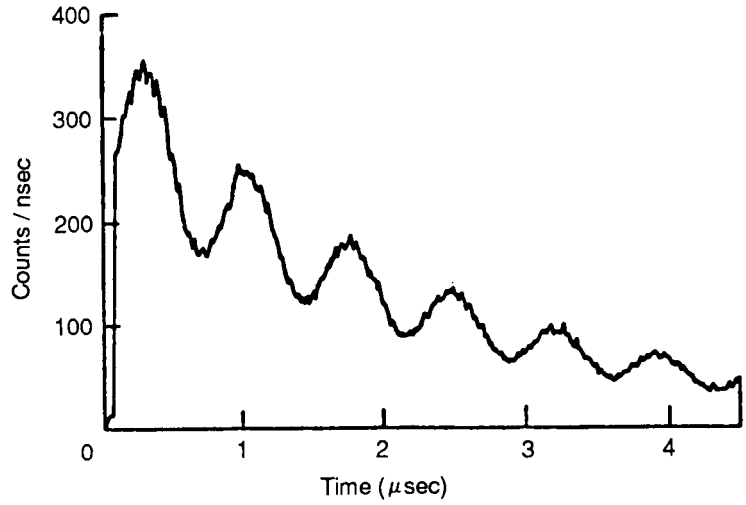

(b) CCl_4 target. (From ref. 41.)

Figure 7. Typical experimental time spectra showing μ^+ precession (μ^+SR) in transverse external field. Number of positron events are plotted against muon residence time in target.

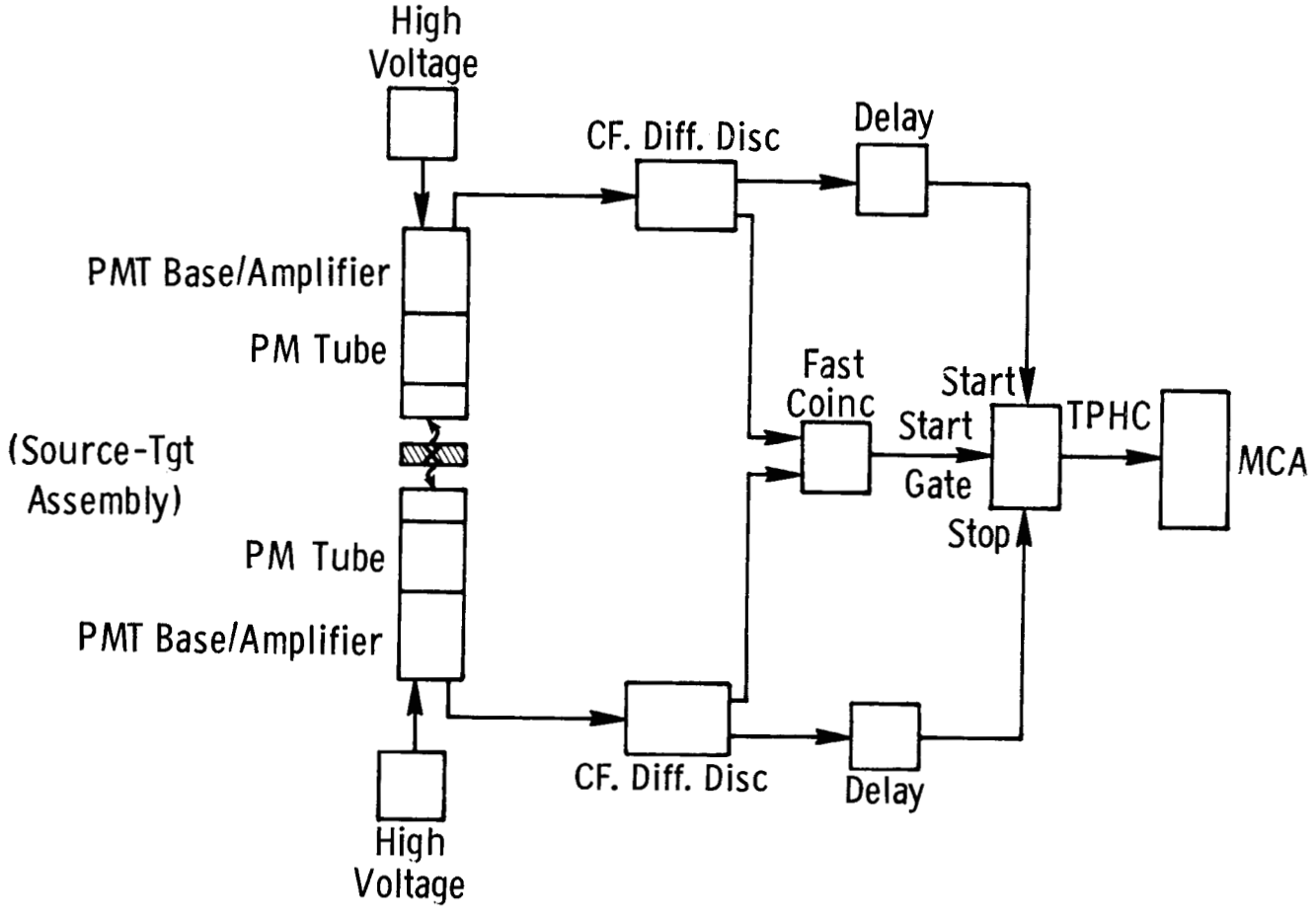

Figure 8. Schematic diagram of fast-positron-lifetime measurement system.

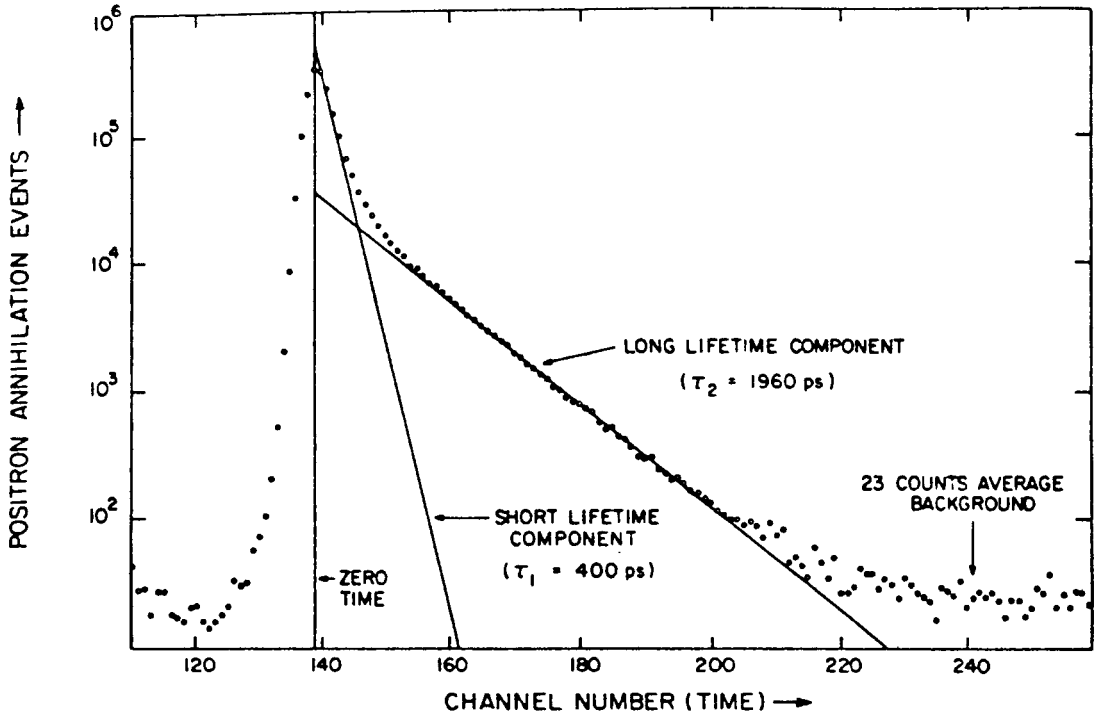

(a) Typical positron lifetime spectrum in dry epoxy specimen.

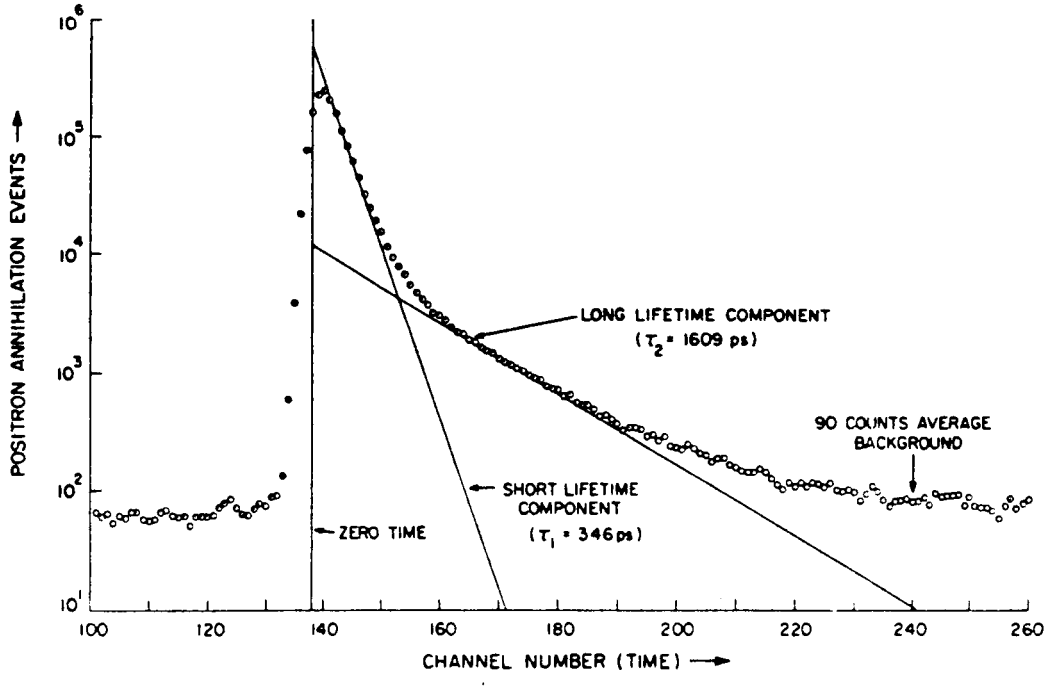

(b) Typical positron lifetime spectrum in dry polyamide specimen.

Figure 9. Typical positron lifetime spectra in polymers.

NASA
National Aeronautics and Space Administration

Report Documentation Page

1. Report No.	2. Government Accession No.	3. Recipient's Catalog No.
NASA RP-1195		

4. Title and Subtitle	5. Report Date
Nuclear Techniques in Studies of Condensed Matter	November 1987
	6. Performing Organization Code
7. Author(s)	8. Performing Organization Report No.
Jag J. Singh	L-16361
9. Performing Organization Name and Address	10. Work Unit No.
NASA Langley Research Center Hampton, VA 23665-5225	505-63-91-01
	11. Contract or Grant No.
12. Sponsoring Agency Name and Address	13. Type of Report and Period Covered
National Aeronautics and Space Administration Washington, DC 20546-0001	Reference Publication
	14. Sponsoring Agency Code

15. Supplementary Notes

16. Abstract

Nuclear techniques have played an important role in the studies of materials over the past several decades. For example, X-ray diffraction, neutron diffraction, neutron activation, and particle- or photon-induced X-ray emission techniques have been used extensively for the elucidation of structural and compositional details of materials. Several new techniques have recently been developed. In this report, we briefly review four techniques which have great potential in the study and development of new materials. Of these four, Mössbauer spectroscopy, muon spin rotation, and positron annihilation spectroscopy techniques exploit their great sensitivity to the local atomic environments in the test materials. Interest in synchrotron radiation, on the other hand, stems from its special properties, such as high intensity, high degree of polarization, and high monochromaticity. It is hoped that this brief review will stimulate interest in the exploitation of these newer techniques for the development of improved materials.

17. Key Words (Suggested by Authors(s))	18. Distribution Statement
Nuclear techniques Materials research Mössbauer spectroscopy Muon spin rotation Positron annihilation spectroscopy Synchrotron radiation research	Unclassified—Unlimited Subject Category 73

19. Security Classif.(of this report)	20. Security Classif.(of this page)	21. No. of Pages	22. Price
Unclassified	Unclassified	19	A02

NASA FORM 1626 OCT 86 NASA-Langley, 1987
For sale by the National Technical Information Service, Springfield, Virginia 22161-2171